Inorg. Chem. **2005**, *44*, 884–895

Examining the Out-of-Center Distortion in the $[NbOF_5]^{2-}$ Anion

Heather K. Izumi, Janet E. Kirsch, Charlotte L. Stern, and Kenneth R. Poeppelmeier*

Department of Chemistry, Northwestern University, Evanston, Illinois 60208-3113

Received September 2, 2004

Out-of-center "primary" electronic distortions are inherent to the oxide fluoride anions of the early d^0 transition metals. In the $[NbOF_5]^{2-}$ anion, the Nb^{5+} moves from the center of the octahedron toward the oxide ligand to form a short Nb═O bond and long trans Nb–F bond. The combined results of single-crystal X-ray diffraction and electronic structure calculations indicate that the primary distortion of the $[NbOF_5]^{2-}$ anion is affected by the coordination environment that is created by the three-dimensional extended structure. The formation of bonds between an $M(L)_4^{2+}$ ($M = Cd^{2+}$, Cu^{2+}; L = 3-aminopyridine, 4-aminopyridine) cation and the oxide and/or *trans*-fluoride ligands of the $[NbOF_5]^{2-}$ anion weakens the π component of the Nb═O bond. At the same time, hydrogen bond interactions between the *equatorial* fluorides and the aminopyridine groups both lengthen the *equatorial* Nb–F bonds and can further reduce the symmetry of the $[NbOF_5]^{2-}$ anion. These combined three-dimensional bond network interactions that serve to lengthen the Nb═O bond and thereby decrease the primary distortion of the $[NbOF_5]^{2-}$ anion are illustrated in the structures of three new niobium oxide fluoride phases, $[4\text{-apyH}]_2[Cu(4\text{-apy})_4(NbOF_5)_2]$ (4-apy = 4-aminopyridine), $Cd(3\text{-apy})_4NbOF_5$ (3-apy = 3-aminopyridine), and $Cu(3\text{-apy})_4NbOF_5$, that were synthesized and characterized using X-ray diffraction. Crystal data for $[4\text{-apyH}]_2[Cu(4\text{-apy})_4(NbOF_5)_2]$: tetragonal, space group $I4_1/acd$ (No. 142), with $a = 20.8745(8)$ Å, $c = 17.2929(9)$ Å, and $Z = 8$. $Cd(3\text{-apy})_4NbOF_5$: tetragonal, space group $P4_3$ (No. 78), with $a = 8.4034(4)$ Å, $c = 34.933(3)$ Å, and $Z = 4$. $Cu(3\text{-apy})_4NbOF_5$: monoclinic, space group $P2_1/n$ (No. 14), with $a = 8.822(1)$ Å, $b = 16.385(3)$ Å, $c = 8.902(1)$ Å, $\beta = 109.270(3)°$, and $Z = 2$.

Introduction

Early work with metal oxide−fluoride systems began with fluoride substitution into solid-state metal oxide phases. The more ionic nature of the metal−fluoride bond was shown to decrease the synthesis, sintering, melting, and Curie temperatures of the resulting compounds.[1] Octahedrally coordinated early d^0 transition metals with the general formula $[MO_xF_{6-x}]^{2-}$ ($x = 1$ or 2) are also of interest because of their distorted octahedral environment. The metal cation at the center of the oxide fluoride octahedron spontaneously moves toward either the corner ($x = 1$) or edge ($x = 2$) occupied by the oxide ligand(s) to form short M═O bonds. This out-of-center "primary" distortion is inherent to the oxide fluoride anions and arises from $d\pi-p\pi$ metal−oxide orbital interactions.[2] For anions of the type $[MOF_5]^{2-}$ (M = Nb, Ta), the central metal distorts toward the single oxide, and a short apical M═O bond and long trans M−F bond are observed in the crystal structure. This distortion leaves an unequal amount of residual negative charge on each ligand; the most anionic ligands will preferentially coordinate and thereby "direct" coordination within the structure. In the $[NbOF_5]^{2-}$ anion, the oxide and *trans*-fluoride retain the most negative charge and, therefore, direct coordination in a trans fashion.[3−5] Alternatively, in $[MoO_2F_4]^{2-}$, the fluorides opposite the oxide ligands retain the most negative charge, and the anion is a cis director.[6−8]

The cis- or trans-directing properties of different $[MO_xF_{6-x}]^{2-}$ anions can be exploited when designing new materials with specific structure-related properties. Second-harmonic generation (SHG) nonlinear optical (NLO) materials belong to one such class with a strict structure−property

* Author to whom correspondence should be addressed. E-mail: krp@northwestern.edu.

(1) Simon, A.; Ravez, J. *Ferroelectrics* **1980**, *24*, 305−307.
(2) Kunz, M.; Brown, I. D. *J. Solid State Chem.* **1995**, *115*, 395−406.
(3) Halasyamani, P.; Willis, M. J.; Heier, K. R.; Stern, C. L.; Poeppelmeier, K. R. *Acta Crystallogr., Sect. C* **1996**, *52*, 2491−2493.
(4) Halasyamani, P.; Willis, M. J.; Stern, C. L.; Lundquist, P. M.; Wong, G. K.; Poeppelmeier, K. R. *Inorg. Chem.* **1996**, *35*, 1367−1371.
(5) Norquist, A. J.; Stern, C. L.; Poeppelmeier, K. R. *Inorg. Chem.* **1999**, *38*, 3448−3449.
(6) Heier, K. R.; Norquist, A. J.; Wilson, C. G.; Stern, C. L.; Poeppelmeier, K. R. *Inorg. Chem.* **1998**, *37*, 76−80.
(7) Maggard, P. A.; Stern, C. L.; Poeppelmeier, K. R. *J. Am. Chem. Soc.* **2001**, *123*, 7742−7743.
(8) Maggard, P. A.; Kopf, A. L.; Stern, C. L.; Poeppelmeier, K. R.; Ok, K. M.; Halasyamani, P. S. *Inorg. Chem.* **2002**, *41*, 4852−4858.

10.1021/ic048766d CCC: $30.25
Published on Web 01/20/2005

relationship. For a material to be NLO active, it must crystallize in a noncentrosymmetric crystal class, that is, one that lacks an inversion center. Out-of-center octahedral distortions, similar to those observed in oxide fluoride anions, are responsible for the SHG properties of both $LiNbO_3$[9] and $KTiOPO_4$,[10] two industrially important solid-state metal oxides. Thus, oxide fluoride anions themselves are an attractive component for the design and synthesis of new SHG active materials.

To obtain noncentrosymmetric oxide fluoride materials, certain challenges must be overcome. First, the oxide and fluoride ligands must crystallize without crystallographic disorder. Second, the anions must align parallel to each other so that the polar components can combine in an additive fashion. An ideal structure for a maximum SHG response is a linear chain configuration where all the polar groups (the oxide fluoride anions) are aligned parallel. When $[NbOF_5]^{2-}$ crystallizes in a linear chain, however, crystallographic disorder between the oxide and *trans*-fluoride ligands imposes an internal center of symmetry.[4,11] Complete crystallographic order of the $[NbOF_5]^{2-}$ anion has previously been achieved in chains that are helical in nature.[5,7,8]

Although many crystal structures of materials that incorporate oxide fluoride anions are well characterized, important fundamental questions remain about the local order adopted by these compounds. In particular, the crystal structure analyses presented here indicate lattice interactions (referred to here as "secondary" distortions) can have significant effects on the inherent, or primary, distortions of oxide fluoride anions. To investigate these effects more thoroughly, electronic structure calculations have been carried out on experimentally obtained results. The results of these calculations provide quantitative support to some of the current hypotheses[12,13] related to the structures of oxide fluoride anions in different coordination environments.

In this paper, the crystal structures of three new niobium oxide fluoride compounds are presented and discussed. $[4\text{-apyH}]_2[Cu(4\text{-apy})_4(NbOF_5)_2]$ (4-apy = 4-aminopyridine) is a salt made up of discrete $[Cu(4\text{-apy})_4(NbOF_5)_2]^{2-}$ "cluster" units, while both $Cd(3\text{-apy})_4NbOF_5$ and $Cu(3\text{-apy})_4NbOF_5$ (3-apy = 3-aminopyridine) have a one-dimensional linear chain structure. $Cd(3\text{-apy})_4NbOF_5$ crystallizes in the noncentrosymmetric, chiral, and polar space group $P4_3$, and $Cu(3\text{-apy})_4NbOF_5$ crystallizes in the centrosymmetric space group $P2_1/n$.

Experimental Section

Caution. Pyridinium poly(hydrogen fluoride) and hydrofluoric acid are toxic and corrosive, and must be handled with extreme caution and the appropriate protective gear! If contact with the liquid or vapor occurs, proper treatment procedures should immediately be followed.[14−16]

Materials. CdO (99.99+%, Aldrich), CuO (99+%, Aldrich), Nb_2O_5 (99.9%, Aldrich), 3-aminopyridine (99%, Aldrich), 4-aminopyridine (98%, Aldrich), pyridinium poly(hydrogen fluoride) [$(HF)_x$·py] (70% HF by weight, Aldrich), and aqueous hydrofluoric acid (HF) (49% HF by weight, Fisher) were used as received.

Synthesis. All reactants were sealed in Teflon [fluoro(ethylene−propylene)] "pouches."[17] The pouches were placed in a Parr pressure vessel filled 33% with deionized H_2O as backfill. The pressure vessel was heated for 24 h at 150 °C and cooled to room temperature over an additional 24 h. The pouches were opened in air, and the products were recovered by vacuum filtration.

$[4\text{-apyH}]_2[Cu(4\text{-apy})_4(NbOF_5)_2]$. $[4\text{-apyH}]_2[Cu(4\text{-apy})_4(NbOF_5)_2]$ was synthesized by reacting 0.0148 g (1.864×10^{-4} mol) of CuO, 0.0248 g (9.322×10^{-5} mol) of Nb_2O_5, 0.3006 g (3.194×10^{-3} mol) of 4-aminopyridine, 0.1257 g (6.282×10^{-3} mol) of 49% aqueous HF, and 0.0179 g (9.933×10^{-4} mol) of deionized H_2O in a 250 mL pressure vessel with up to six other pouches. Blue needles were recovered in 40% yield based on CuO.

Aqueous hydrofluoric acid was used in place of $(HF)_x$·py to avoid coordination of pyridine to copper. 4-Aminopyridine is more basic ($pK_a = 9.11$) than pyridine ($pK_a = 5.25$) and would readily protonate, leaving neutral pyridine to form the $[Cu(py)_4]^{2+}$ cation.

$Cd(3\text{-apy})_4NbOF_5$. $Cd(3\text{-apy})_4NbOF_5$ was synthesized by reacting 0.0501 g (3.902×10^{-4} mol) of CdO, 0.0508 g (1.911×10^{-4} mol) of Nb_2O_5, 1.0008 g (1.063×10^{-2} mol) of 3-aminopyridine, 0.3985 g (1.513×10^{-3} mol) of $(HF)_x$·py, and 0.1015 g (5.633×10^{-3} mol) of deionized H_2O in a 2 L pressure vessel with up to 20 other pouches. Clear, colorless needles of $Cd(3\text{-apy})_4NbOF_5$ were recovered in low yield with polycrystalline CdF_2. No other crystalline phases were isolated in the composition space.[4,11,18]

$Cu(3\text{-apy})_4NbOF_5$. $Cu(3\text{-apy})_4NbOF_5$ was synthesized by reacting 0.0298 g (3.748×10^{-4} mol) of CuO, 0.0498 g (1.874×10^{-4} mol) of Nb_2O_5, 0.9940 g (1.056×10^{-2} mol) of 3-aminopyridine, 0.0929 g (3.527×10^{-4} mol) of $(HF)_x$·py, and 0.1172 g (6.504×10^{-3} mol) of deionized H_2O in a 2 L pressure vessel with up to 20 other pouches. Blue needles were recovered in 80% yield based on CuO. No other crystalline phases were isolated in the composition space.

Crystallographic Determination. Single-crystal X-ray diffraction data were collected with Mo Kα radiation ($\lambda = 0.71073$ Å) on a Bruker SMART-1000 CCD diffractometer and integrated with the SAINT-Plus program.[19] The structures were solved by direct methods and refined by full-matrix least-squares techniques.[20] A face-indexed absorption correction was performed numerically using the program XPREP. The Flack parameter was used to verify the absolute structure of $Cd(3\text{-apy})_4NbOF_5$.[21] The shorter bond distance between the two bridging positions (oxygen and the *trans*-fluorine) was assigned to the Nb−O bond. Models that mix oxygen and fluorine on these two general positions are, of course, indistinguishable. All structures were checked for missing symmetry elements

(9) Matthias, B. T.; Remeika, J. P. *Phys. Rev.* **1949**, *76*, 1886.
(10) Zumsteg, F. C.; Bierlein, J. D.; Gier, T. E. *J. Appl. Phys.* **1976**, *47*, 4980−4985.
(11) Halasyamani, P. S.; Heier, K. R.; Norquist, A. J.; Stern, C. L.; Poeppelmeier, K. R. *Inorg. Chem.* **1998**, *37*, 369−371.
(12) Heier, K. R.; Poeppelmeier, K. R. *J. Solid State Chem.* **1997**, *133*, 576−579.
(13) Du, L.-S.; Schurko, R. W.; Kim, N.; Grey, C. P. *J. Phys. Chem. A* **2002**, *106*, 7876−7886.
(14) Bertolini, J. C. *J. Emerg. Med.* **1992**, *10*, 163−168.
(15) Peters, D.; Miethchen, R. *J. Fluorine Chem.* **1996**, *79*, 161−165.
(16) Segal, E. B. *Chem. Health Saf.* **2000**, *7*, 18−23.
(17) Harrison, W. T. A.; Nenoff, T. M.; Gier, T. E.; Stucky, G. D. *Inorg. Chem.* **1993**, *32*, 2437−2441.
(18) Norquist, A. J.; Heier, K. R.; Stern, C. L.; Poeppelmeier, K. R. *Inorg. Chem.* **1998**, *37*, 6495−6501.
(19) *SAINT-Plus*; Bruker Analytical X-ray Instruments, Inc.: Madison, WI, 2000.
(20) Sheldrick, G. M. *SHELXTL*, version 5.10; Bruker Analytical X-ray Instruments, Inc.: Madison, WI, 1997.
(21) Flack, H. D. *Acta Crystallogr., Sect. A* **1983**, *39*, 876−881.

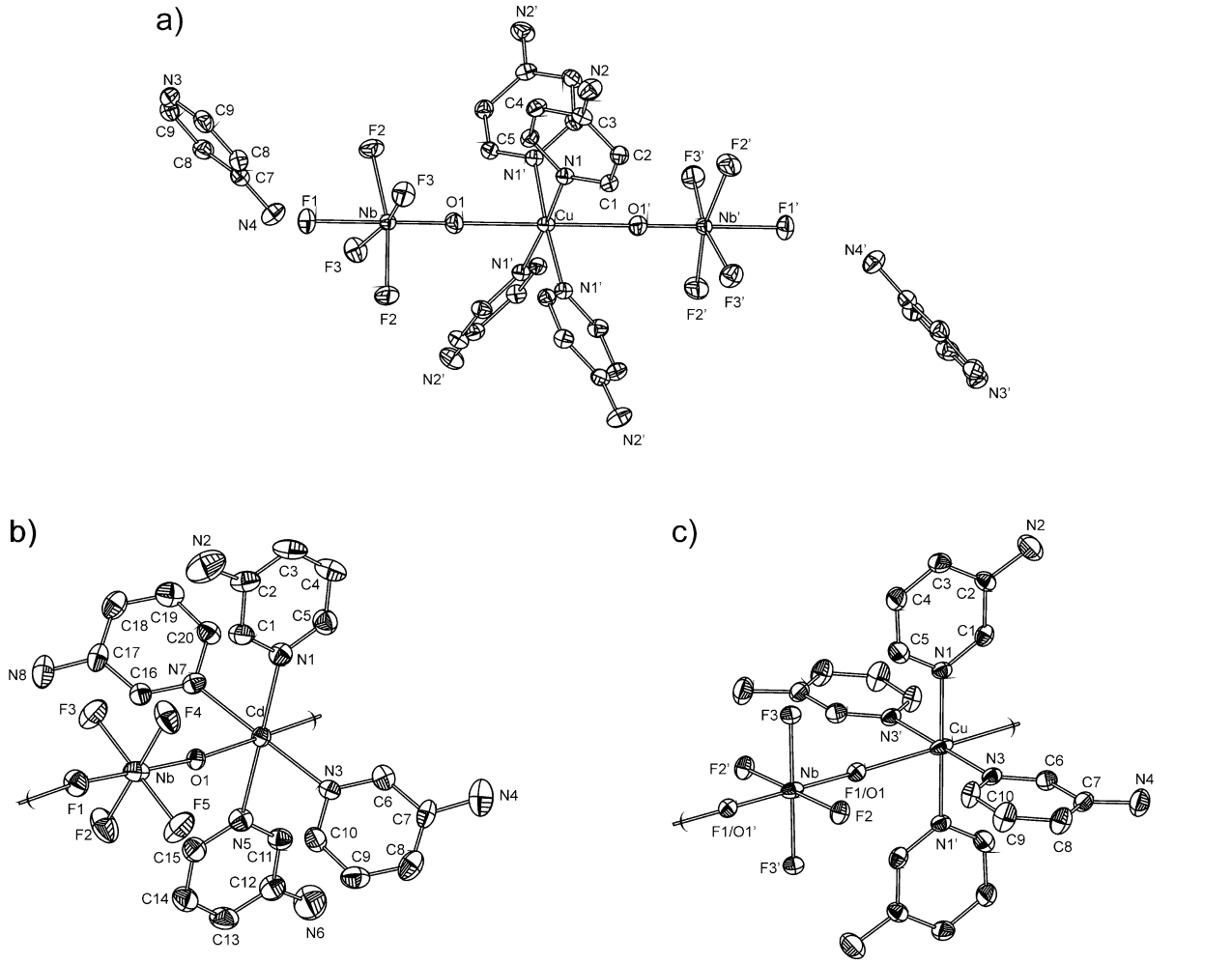

Figure 1. Thermal ellipsoid plots (showing 50% probability) of (a) $[4\text{-apyH}]_2[Cu(4\text{-apy})_4(NbOF_5)_2]$, (b) $Cd(3\text{-apy})_4NbOF_5$, and (c) $Cu(3\text{-apy})_4NbOF_5$.

with PLATON.[22] The final refinement includes anisotropic displacement parameters for the non-hydrogen atoms. Hydrogen atoms were placed in calculated positions (C−H = 0.95 Å and N−H = 0.88 Å) and were refined using a riding model with isotropic displacement parameters constrained to equal 1.2 times the equivalent isotropic displacement parameter of the parent atom. See Figure 1 for thermal ellipsoid plots, Table 1 for crystallographic data, and the Supporting Information for X-ray crystallographic files of each compound.

Spectroscopic Measurements. Mid-infrared (400−4000 cm^{-1}) spectra were collected using a Bio-Rad FTS-60 FTIR spectrometer operating at 2 cm^{-1} resolution.

Nonlinear Optical Measurements. The powder SHG measurement of $Cd(3\text{-apy})_4NbOF_5$ was performed on a modified Kurtz−NLO system using 1064 nm light and the previously published methods.[23]

Computational Study. Electronic structure calculations based on the crystallographically determined coordinates for molecular fragments of the $Cd(3\text{-apy})_4NbOF_5$ linear chain and the $[pyH]_2[Cd(py)_4(NbOF_5)_2]$ "cluster"[3] structures, as well as the uncoordinated, DFT-optimized $[NbOF_5]^{2-}$ anion,[24] were all carried out using the Fenske−Hall molecular orbital method.[25] A truncated chain unit

Table 1. Crystallographic Data for $[4\text{-apyH}]_2[Cu(4\text{-apy})_4(NbOF_5)_2]$, $Cd(3\text{-apy})_4NbOF_5$, and $Cu(3\text{-apy})_4NbOF_5$

	$[4\text{-apyH}]_2[Cu(4\text{-apy})_4(NbOF_5)_2]$	$Cd(3\text{-apy})_4NbOF_5$	$Cu(3\text{-apy})_4NbOF_5$
formula	$C_{30}H_{38}CuF_{10}N_{12}Nb_2O_2$	$C_{20}H_{24}CdF_5N_8NbO$	$C_{20}H_{24}CuF_5N_8NbO$
fw	1038.08	692.78	643.91
space group	$I4_1/acd$ (No. 142)	$P4_3$ (No. 78)	$P2_1/n$ (No. 14)
a (Å)	20.8745(8)	8.4034(4)	8.822(1)
b (Å)	20.8745(8)	8.4034(4)	16.385(3)
c (Å)	17.2929(9)	34.933(3)	8.902(1)
β (°)	90	90	109.270(3)
V (Å^3)	7535.3(6)	2466.9(2)	1214.7(3)
Z	8	4	2
T (°C)	−120(1)	−120(1)	−120(1)
λ (Å)	0.71069	0.71069	0.71069
ρ_{calc} (g/cm^3)	1.830	1.865	1.760
ρ_{obsd}[a] (g/cm^3)	1.83(7)	1.884(8)	1.731(3)
μ (cm^{-1})	12.55	13.95	14.16
$R(F)$[b]	0.0339	0.0406	0.0317
wR2(F^2)[c]	0.0807	0.0947	0.0779
Flack parameter		−0.02(3)	

[a] Density measurements by flotation pycnometry at 25 °C. [b] $R = \sum|F_o| - |F_c||/\sum|F_o|$. [c] $wR2 = [\sum w(F_o^2-F_c^2)^2/\sum w(F_o^2)^2]^{1/2}$.

(22) Spek, A. L. *PLATON*; Utrecht University: Utrecht, The Netherlands, 2001.
(23) Porter, Y.; Ok, K. M.; Bhuvanesh, N. S. P.; Halasyamani, P. S. *Chem. Mater.* **2001**, *13*, 1910−1915.
(24) Welk, M. E.; Norquist, A. J.; Arnold, F. P.; Stern, C. L.; Poeppelmeier, K. R. *Inorg. Chem.* **2002**, *41*, 5119−5125.

Table 2. Selected Bond Lengths (Å) and Bond Valence Sums[a,b] of $[NbOF_5]^{2-}$

bond	R_i, Å	S_i	$V_i - S_i$	bond	Å
$[4\text{-apy}]_2[Cu(4\text{-apy})_4(NbOF_5)_2]$				**$Cu(3\text{-apy})_4NbOF_5$**	
Nb═O1	1.730(3)	1.63	0.37	Nb−F1/O1 × 2	1.919(1)
Nb−F1	2.118(2)	0.45	0.55	Nb−F2 × 2	1.940(1)
Nb−F2 × 2	1.945(2)	0.72	0.28	Nb−F3 × 2	1.942(1)
Nb−F3 × 2	1.950(2)	0.71	0.29		
	ΣS_{Nb}	4.94		Cu−F1/O1 × 2	2.532(1)
				Cu−N1 × 2	2.034(1)
Cu−O1× 2	2.402(3)			Cu−N3 × 2	2.027(1)
Cu−N1× 4	2.030(2)				
$Cd(3\text{-apy})_4NbOF_5$					
Nb═O1	1.914(3)	0.99	1.01		
Nb−F1	1.937(3)	0.73	0.27		
Nb−F2	1.914(4)	0.78	0.22		
Nb−F3	1.913(4)	0.78	0.22		
Nb−F4	1.931(4)	0.75	0.25		
Nb−F5	1.905(4)	0.80	0.20		
	ΣS_{Nb}	4.83			
Cd−O1	2.278(3)				
Cd−F1	2.288(3)				
Cd−N1	2.328(4)				
Cd−N3	2.335(4)				
Cd−N5	2.338(4)				
Cd−N7	2.329(4)				

[a] Bond valence calculated with the program Bond Valence Calculator version 2.00, Hormillosa, C., Healy, S., Stephen, T. McMaster University, 1993. [b] Valence sums calculated with the formula: $S_i = \exp[(R_0 - R_i)/B]$, where S_i = valence of bond "*i*", R_0 = constant dependent on the bonded elements, R_i = bond length of bond "*i*", and $B = 0.370$. ΣS_{Nb} = bond valence sum for the metal. V_i = oxidation state for each ligand. $V_i - S_i$ = calculated charge of the ligand. R_0(Nb═O) = 1.911, R_0(Nb−F) = 1.822.

consisting of three $[NbOF_5]^{2-}$ anions alternating with two $[Cd(3\text{-apy})_4]^{2+}$ cations served as a model for $Cd(3\text{-apy})_4NbOF_5$, while the $[pyH]_2[Cd(py)_4(NbOF_5)_2]$ cluster was modeled by a single $[NbOF_5][Cd(py)_4][NbOF_5]^{2-}$ unit. See Supporting Information for atomic coordinates. Atomic charges and overlap populations were calculated via Mulliken population analyses.[26,27]

All atomic basis functions were obtained by a best fit to Herman−Skillman atomic calculations[28] using the method of Bursten, Jensen, and Fenske.[29] The 5s and 5p functions were given exponents of 2.2 for Nb and Cd. Valence 2p functions for C, N, O, and F were retained as double-ζ functions, while all other functions were reduced to single-ζ functions. Hydrogen was assigned an exponent of 1.2.

Results

$[4\text{-apyH}]_2[Cu(4\text{-apy})_4(NbOF_5)_2]$. $[4\text{-apyH}]_2[Cu(4\text{-apy})_4(NbOF_5)_2]$ is composed of a central $Cu(4\text{-apy})_4^{2+}$ cation with four short equatorial Cu−N bonds at 2.030(2) Å × 4. $Cu(4\text{-apy})_4^{2+}$ is coordinated to two $[NbOF_5]^{2-}$ anions through long axial Cu−O bonds of 2.402(3) Å to complete the anionic "cluster" $[Cu(4\text{-apy})_4(NbOF_5)_2]^{2-}$. Selected bond lengths are listed in Table 2. For each cluster, there are two $[4\text{-apyH}]^+$ cations that serve both as charge balance and as hydrogen bond donors. The clusters of $[Cu(4\text{-apy})_4(NbOF_5)_2]^{2-}$ pack end-to-end in a zigzag arrangement in the *ab* planes; each subsequent layer is rotated by 90°. The $[4\text{-apyH}]^+$ cations lie in the *ac* and *bc* planes around the 4_1-screw axis. See Figure 2a.

All five fluorides of the $[NbOF_5]^{2-}$ anion hydrogen bond to 4-aminopyridine rings of the $[Cu(4\text{-apy})_4]^{2+}$ or $[4\text{-apyH}]^+$ cations. The *trans*-fluoride, F1, hydrogen bonds to the amino group of two $[4\text{-apyH}]^+$ cations at d(N4−H···F1) = 2.752 Å × 2. The amino group from a 4-aminopyridine ring of a neighboring cluster and the acidic proton of a $[4\text{-apyH}]^+$ cation both hydrogen bond to F2 at d(N2−H···F2) = 2.928 Å and d(N3−H···F2) = 2.778 Å, respectively, while F3 is bound to one amino group of a neighboring cluster at d(N2−H···F3) = 2.896 Å. See Figure 2b.

The infrared spectrum shows a characteristic band for $[NbOF_5]^{2-}$ at ν_s(Nb═O) = 916 cm^{-1}. Additional bands at 3444, 3356, 1652, 1619, 1519, 1213, and 1020 cm^{-1} are indicative of 4-aminopyridine coordinated to copper.[30]

$Cd(3\text{-apy})_4NbOF_5$. The one-dimensional linear chain structure of $Cd(3\text{-apy})_4NbOF_5$ is comprised of alternating $[NbOF_5]^{2-}$ anions and $Cd(3\text{-apy})_4^{2+}$ cations. See Figure 3a. The d^{10} Cd^{2+} forms four equatorial bonds to the "soft" 3-aminopyridine rings at distances of Cd−N1 = 2.328(4) Å, Cd−N3 = 2.335(4) Å, Cd−N5 = 2.338(4) Å, and Cd−N7 = 2.329(4) Å. The axial positions of the cation are occupied by a bridging oxide and fluoride at 2.278(3) and 2.288(3) Å, respectively. These bridging ligands also make a "short" Nb═O and "long" trans Nb−F bond to Nb^{5+} at Nb═O1 = 1.914(3) Å and Nb−F1 = 1.937(3) Å. Four equatorial fluoride ligands complete the coordination sphere around Nb^{5+} at lengths of Nb−F2 = 1.914(4) Å, Nb−F3 = 1.913(4) Å, Nb−F4 = 1.931(4) Å, and Nb−F5 = 1.905(4) Å. Bond lengths are listed in tabular format in Table 2. In each chain, the $[NbOF_5]^{2-}$ anions are oriented in a polar fashion; this results in linear chains that have a net dipole moment. The chains are aligned parallel to each other in the *ab* plane. A 4_3-screw axis rotates the sheet by 90° every *c*/4. See Figure 4a.

Three of the four $[NbOF_5]^{2-}$ equatorial fluorides, F2, F3, and F4, hydrogen bond with an amino group from surrounding 3-aminopyridine rings. F2 forms two hydrogen bonds, one at d(N2−H···F2) = 2.917 Å to a ring on a chain in the same sheet and one d(N4−H···F2) = 3.088 Å to a ring in a neighboring sheet, as shown in Figure 4b. F3 accepts a hydrogen from a chain in an adjacent sheet d(N6−H···F3) = 2.942 Å. F4 hydrogen bonds to a chain in the same sheet at d(N8−H···F4) = 3.080 Å and a chain in an adjacent sheet d(N6−H···F4) = 3.167 Å. The fourth fluoride, F5, does not participate in hydrogen bonding.

The infrared spectrum of $Cd(3\text{-apy})_4NbOF_5$ confirms the presence of the $[NbOF_5]^{2-}$ anion with a strong peak observed at ν_s(Nb═O) = 890 cm^{-1}.[31,32] Additional peaks at 3456, 3371, 1625, 1490, and 1445 cm^{-1} are characteristic of 3-aminopyridine coordinated to cadmium.[33]

(25) Hall, M. B.; Fenske, R. F. *Inorg. Chem.* **1972**, *11*, 768−775.
(26) Mulliken, R. S. *J. Chem. Phys.* **1955**, *23*, 1833−1840.
(27) Mulliken, R. S. *J. Chem. Phys.* **1955**, *23*, 1841−1846.
(28) Herman, F.; Skillman, S. *Atomic Structure Calculations*; Prentice Hall: Englewood Cliffs, NJ, 1963.
(29) Bursten, B. E.; Jensen, J. R.; Fenske, R. F. *J. Chem. Phys.* **1978**, *68*, 3320−3321.
(30) Akyuz, S. *J. Mol. Struct.* **1999**, *482*−*483*, 171−174.
(31) Keller, O. J., Jr. *Inorg. Chem.* **1963**, *2*, 783−787.
(32) Pausewang, G.; Schmitt, R.; Dehnicke, K. *Z. Anorg. Allg. Chem.* **1974**, *408*, 1−8.
(33) Akyuz, S. *J. Mol. Struct.* **1998**, *449*, 23−27.

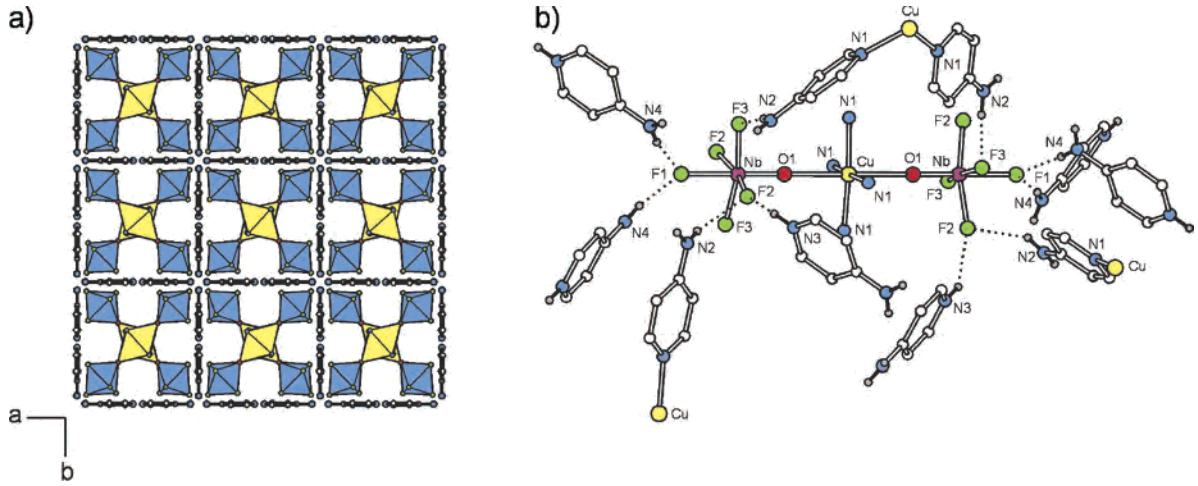

Figure 2. (a) Three-dimensional packing of $[4\text{-apyH}]_2[Cu(4\text{-apy})_4(NbOF_5)_2]$. Blue polyhedra represent $[NbOF_5]^{2-}$, and yellow polyhedra represent $Cu(4\text{-apy})_4^{2+}$ and (b) the hydrogen bond environment around the $[NbOF_5]^{2-}$ anion. N1 is the ring nitrogen and N2 is the amino group nitrogen of the coordinated 4-aminopyridine rings of $Cu(4\text{-apy})_4^{2+}$. N3 is the ring nitrogen and N4 is the amino group nitrogen of $[4\text{-apyH}]^+$. Ring hydrogens have been removed for clarity.

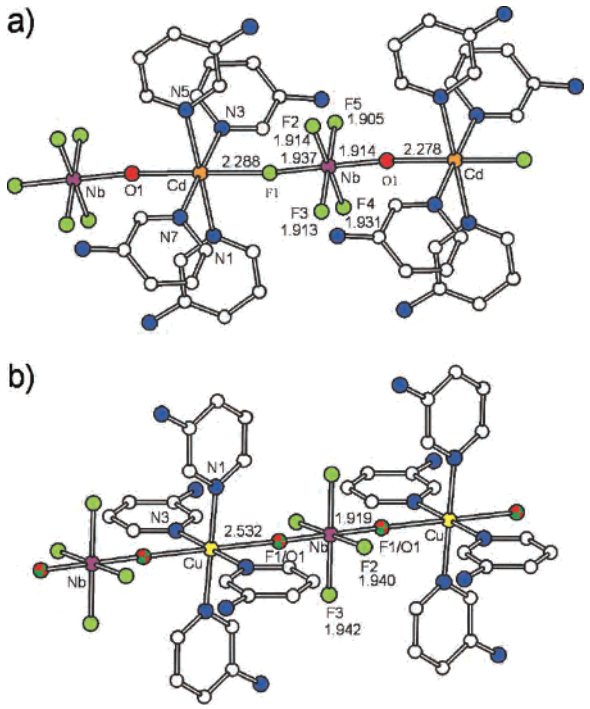

Figure 3. Linear chains of (a) $Cd(3\text{-apy})_4NbOF_5$ and (b) $Cu(3\text{-apy})_4NbOF_5$.

$Cu(3\text{-apy})_4NbOF_5$. When Cd^{2+} is replaced by Cu^{2+}, the resulting $Cu(3\text{-apy})_4NbOF_5$ compound crystallizes with similar one-dimensional linear chains, as shown in Figure 3b. Unlike $Cd(3\text{-apy})_4NbOF_5$, however, all the chains of $Cu(3\text{-apy})_4NbOF_5$ align parallel to the *c* axis. See Figure 5a. The d^9 Jahn−Teller distorted $Cu(3\text{-apy})_4^{2+}$ cation exhibits a tetragonal elongation, with four short equatorial bonds made to 3-aminopyridine rings at Cu−N1 = 2.034(2) Å × 2 and Cu−N3 = 2.027(2) Å × 2. The location of Cu^{2+} and Nb^{5+} on inversion centers requires two identical bridging axial positions. Occupancy of the bridging positions is fixed at 0.5 O and 0.5 F, with an averaged Cu−O/F bond distance of 2.53 Å and an averaged Nb−O/F bond distance of 1.919(1) Å. The four equatorial fluoride bonds are observed at Nb−F2 = 1.940(1) Å × 2 and Nb−F3 = 1.942(1) Å × 2. Selected bond lengths are given in Table 2.

Hydrogen bonding occurs between all four equatorial fluorides of the $[NbOF_5]^{2-}$ anion and an amino group from a $Cu(3\text{-apy})_4^{2+}$ cation in four surrounding linear chains. As shown in Figure 5b, two of these cations are in the same *ab* plane as the anion and are trans to each other with *d*(N2−H···F2) = 3.089 Å × 2. The other two cations are located in the sheet below and another in the sheet above the anion at *d*(N4−H···F3) = 3.133 Å × 2.

The infrared spectrum shows a characteristic band for $[NbOF_5]^{2-}$ at ν_s(Nb═O) = 891 cm^{-1} and bands at 3414, 3327, 1619, 1490, and 1446 cm^{-1} that correspond to 3-aminopyridine rings coordinated to copper.[33]

Calculations. Rather than carrying out full solid-state band structure calculations, discrete molecular fragments of the oxide fluoride compounds have served as models in the computational studies presented here. This approximation is similar to the finite-cluster approximation that is frequently made in computational studies of adsorbate-covered surfaces.[34,35] Models for the linear chain compounds consisted of five octahedra (three anions alternated with two cations). At this size, the effects of chain termination are less significant than on smaller models, yet the chain is still short enough to keep the number of basis functions tractable.

Another approximation made in these computational studies was the use of the Fenske−Hall (FH) method[25] for characterizations of the bonding and electronic structure of the oxide fluoride molecular fragments. The FH method is a self-consistent, approximate Hartree−Fock method. Owing to the inherent approximations made by the FH approach that do not allow for the evaluation of total energies, *geometry optimization is not possible with this method*. The

(34) Johnson, B. F. G.; Gallup, M.; Roberts, Y. V. *J. Mol. Catal.* **1994**, *86*, 51−69.
(35) Koper, M. T. M.; Van Santen, R. A.; Neurock, M. Theory and Modeling of Catalytic and Electrocatalytic Reactions. In *Catalysis and Electrocatalysis at Nanoparticle Surfaces*; Wieckowski, A., Savinova, E. R., Vayenas, C. G., Eds.; Marcel Dekker: New York, 2003; pp 1−34.

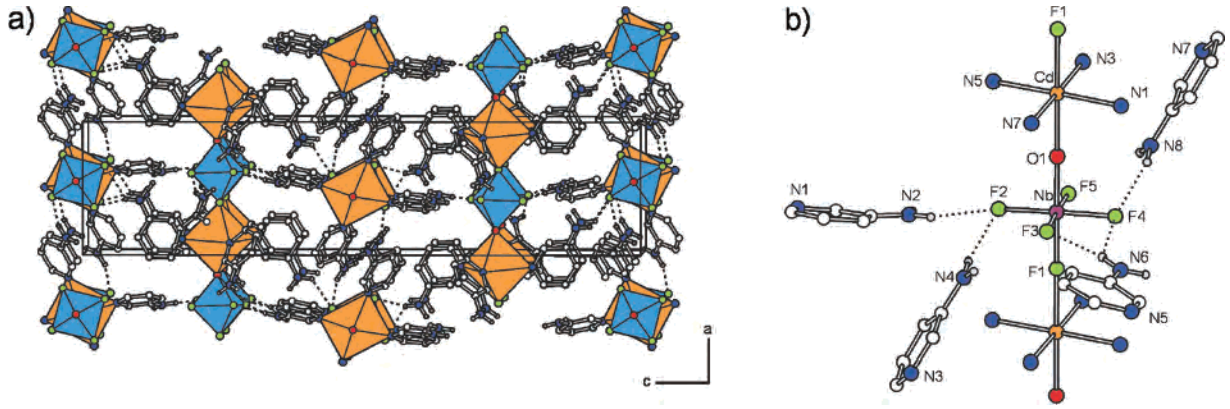

Figure 4. (a) Three-dimensional packing of $Cd(3\text{-apy})_4NbOF_5$. Blue polyhedra represent $[NbOF_5]^{2-}$ and orange polyhedra represent $Cd(3\text{-apy})_4^{2+}$ and (b) the asymmetric hydrogen bond environment around the $[NbOF_5]^{2-}$ anion. Ring hydrogens have been removed for clarity.

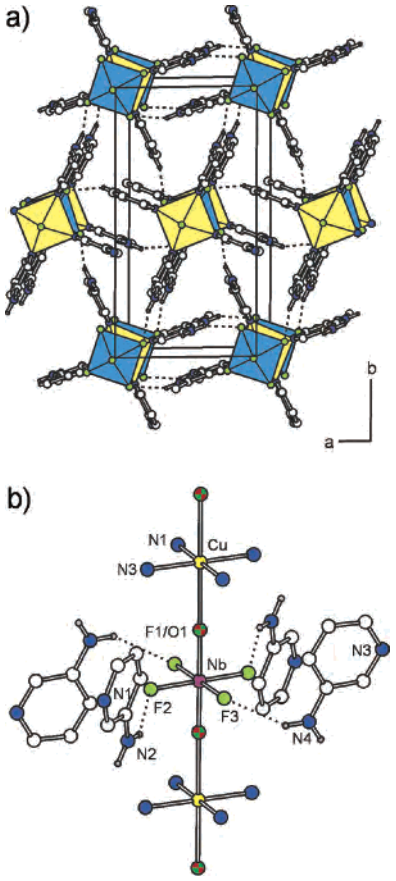

Figure 5. (a) Three-dimensional packing of $Cu(3\text{-apy})_4NbOF_5$. Blue polyhedra represent $[NbOF_5]^{2-}$ and yellow polyhedra represent $Cu(3\text{-apy})_4^{2+}$ and (b) the symmetric hydrogen bond environment around the $[NbOF_5]^{2-}$ anion. Ring hydrogens have been removed for clarity.

results of FH calculations, however, provide a reliable and detailed description of the bonding environment of any atom in the molecular fragment. Also, use of the FH method generated results for the large systems discussed below within a reasonable amount of computational time and resources.

Finally, although there are many different methods used in the assignation of electronic populations and charges in computational studies, the systems described in this paper are compared using Mulliken population analyses.[26,27] In this methodology, electronic charges are assigned according to the atomic orbital coefficients of normalized molecular wave functions that are represented as linear combinations of atomic orbitals (LCAOs). Despite the simplicity of Mulliken analyses, they provide a sufficient level of accuracy in describing general trends exhibited by the closely related structures compared below.

Discussion

The primary distortion within the $[NbOF_5]^{2-}$ anion results in a Nb═O bond that is both stronger and more covalent than the bond between the Nb^{5+} and the more electronegative F^- anions. Weaker "secondary" distortions arise from interactions between the extended three-dimensional bond network and the equatorial fluorides on $[NbOF_5]^{2-}$.[24] The oxide and *trans*-fluoride sites must be ordered within the crystal structure for both types of distortions to be observed. Furthermore, a secondary distortion of the anion can be observed when bond network interactions occur asymmetrically. Bond valence calculations[36,37] can be used to help analyze the coordination effects to the $[NbOF_5]^{2-}$ anion. In general, the $[NbOF_5]^{2-}$ anion obeys the valence sum rule, and the total valence on niobium sums to 5.[2] However, as the asymmetry and number of bond network interactions increase, the valence on niobium deviates from that value. An asymmetrically distorted anion is indicated by an atomic valence on niobium that is significantly less than 5.

Cluster Compounds. The "cluster" compounds share a similar 2:1 anion to cation composition. These salts are composed of a central $Cu(L)_4^{2+}$ (L = pyridine, 4-apy) cation and two axially coordinated oxide fluoride anions that form an overall negatively charged discrete unit. The $[LH]^+$ cations both balance the charge and provide an acidic proton for hydrogen bonding. The oxide of the $[NbOF_5]^{2-}$ anion preferentially binds to $M(L)_4^{2+}$, while a hydrogen bond is made between the acidic proton of $[LH]^+$ and the *trans*-fluoride ligand. A primary distortion is observed in the crystallographically ordered anion with a short Nb═O bond, long trans Nb−F bond, and bond angles that deviate from perfect O_h symmetry.

(36) Brown, I. D.; Altermatt, D. *Acta Crystallogr., Sect. B* **1985**, *41*, 244−247.
(37) Brese, N. E.; O'Keeffe, M. *Acta Crystallogr., Sect. B* **1991**, *47*, 192−197.

Table 3. Selected Bond Lengths and Bond Valence Calculations of $[NbOF_5]^{2-}$

bond	R_i, Å	S_i	$V_i - S_i$	bond	R_i, Å	S_i	$V_i - S_i$
	$[pyH]_2[Cu(py)_4(NbOF_5)_2]$				**$[HNC_6H_6OH]_2[Cu(py)_4(NbOF_5)_2]$**		
Nb═O1	1.728(8)	1.64	0.36	Nb═O1	1.763(1)	1.49	0.51
Nb−F1 × 2	1.937(6)	0.73	0.27	Nb−F1	1.936(1)	0.74	0.26
Nb−F2 × 2	1.927(5)	0.75	0.25	Nb−F2	1.912(1)	0.78	0.22
Nb−F3	2.099(8)	0.47	0.53	Nb−F3	1.924(1)	0.76	0.24
	ΣS_{Nb}	5.07		Nb−F4	1.981(1)	0.65	0.35
				Nb−F5	2.098(1)	0.47	0.53
Cu−O1 × 2	2.417(9)				ΣS_{Nb}	4.89	
				Cu−O1 × 2	2.307(2)		
	$[pyH]_2[Cd(py)_4(NbOF_5)_2]$				**$Cu(dpa)_2NbOF_5 \cdot 2H_2O$**		
Nb═O1	1.750(6)	1.55	0.45	Nb═O1	1.760(1)	1.50	0.50
Nb−F1 × 2	1.932(3)	0.74	0.26	Nb−F1	1.953(1)	0.70	0.30
Nb−F2 × 2	1.936(3)	0.74	0.26	Nb−F2	1.923(1)	0.76	0.24
Nb−F3	2.095(4)	0.48	0.52	Nb−F3	1.928(1)	0.75	0.25
	ΣS_{Nb}	4.99		Nb−F4	1.928(1)	0.75	0.25
				Nb−F5	2.072(1)	0.51	0.49
Cd−O1 × 2	2.333(6)				ΣS_{Nb}	4.97	

A comparison between $[4\text{-apyH}]_2[Cu(4\text{-apy})_4(NbOF_5)_2]$ and two previously published cluster compounds, $[pyH]_2[Cu(py)_4(NbOF_5)_2]$[4] and $[HNC_6H_6OH]_2[Cu(py)_4(NbOF_5)_2]$,[24] shows how bond network interactions affect the distortion of the $[NbOF_5]^{2-}$ anion. See Table 3 and the Supporting Information. In $[pyH]_2[Cu(py)_4(NbOF_5)_2]$, the $[NbOF_5]^{2-}$ anions form long bonds of 2.417(9) Å from the oxide to copper. The corresponding Nb═O bond is short at 1.728(8) Å, and strong, as indicated by the high Nb═O bond valence value. The trans Nb−F bond is long and has a low valence, while the equatorial Nb−F bonds are of medium length at 1.937(6) and 1.927(5) Å, resulting in an atomic valence near 5 on niobium.

The cluster compound $[4\text{-apyH}]_2[Cu(4\text{-apy})_4(NbOF_5)_2]$ has Cu−O and Nb═O bond lengths similar to those of $[pyH]_2[Cu(py)_4(NbOF_5)_2]$. Replacement of pyridine with 4-aminopyridine lowers the acidity of the $[LH]^+$ proton by donating electron density into the ring and makes the amino hydrogens more accessible for participation in hydrogen bonding. Consequently, in $[4\text{-apyH}]_2[Cu(4\text{-apy})_4(NbOF_5)_2]$, the hydrogen bond made to the *trans*-fluoride is from an amino group, unlike the other clusters. The increase of hydrogen bond donors in this cluster allows all four equatorial fluorides to participate in hydrogen bonding. In general, hydrogen bonds have been shown to both weaken and lengthen the bond made by the acceptor (an equatorial fluoride) to the atoms in its primary coordination sphere (Nb^{5+}).[38] The equatorial fluoride bonds to Nb^{5+} in $[4\text{-apyH}]_2[Cu(4\text{-apy})_4(NbOF_5)_2]$ are lengthened to 1.945(2) and 1.950(2) Å, which lowers the overall valence on niobium to slightly below 5. The $[NbOF_5]^{2-}$ anion forms the shortest bond to copper in $[HNC_6H_6OH]_2[Cu(py)_4(NbOF_5)_2]$ where the Cu−O bond is 2.307(3) Å in length. The corresponding Nb═O bond length is longer than the previous example at 1.763(1) Å. Only one of the four equatorial fluorides on each $[NbOF_5]^{2-}$ anion participates in hydrogen bonding; this results in a long Nb−F bond at 1.981(1) Å and an observable secondary distortion. The Nb═O and trans Nb−F bonds in $[HNC_6H_6OH]_2[Cu(py)_4(NbOF_5)_2]$ have a lower bond valence than in the other two clusters. The valence on niobium remains below 5.

Asymmetrical bond network interactions with the $[NbOF_5]^{2-}$ anion determine the direction of the distortion.[2] When all four equatorial fluorides form symmetrical hydrogen bonds as in $[4\text{-apyH}]_2[Cu(4\text{-apy})_4(NbOF_5)_2]$, a secondary distortion is unobservable. The asymmetrical contacts to the oxide and *trans*-fluoride, namely the Cu−O bond and the hydrogen bond to fluoride, are the two directional components that affect the distortion of the anion. These contacts are collinear with the primary distortion. In $[HNC_6H_6OH]_2[Cu(py)_4(NbOF_5)_2]$, however, a hydrogen bond is made to only one of four equatorial fluorides. Thus, there are three directional components to the distortion: the Cu−O bond, the *trans*-fluoride hydrogen bond, and the equatorial fluoride−hydrogen bond. This secondary distortion is accompanied by a decrease in symmetry of the $[NbOF_5]^{2-}$ anion.[2] The symmetry of the anion is defined as the approximate symmetry of a $[NbOF_5]^{2-}$ unit in the structure and not the actual crystallographic site symmetry.[24]

The single hydrogen bond made to the equatorial fluoride, F4, in $[HNC_6H_6OH]_2[Cu(py)_4(NbOF_5)_2]$ interferes with the primary distortion of the anion. This secondary distortion lengthens the Nb═O bond by adding an additional directional component to the distortion. The Nb═O bond distance of 1.763(1) Å in $[HNC_6H_6OH]_2[Cu(py)_4(NbOF_5)_2]$ is longer than that in $[4\text{-apyH}]_2[Cu(4\text{-apy})_4(NbOF_5)_2]$, where a secondary distortion is undetectable. The secondary distortion decreases the symmetry of the $[NbOF_5]^{2-}$ anion from approximately C_{4v} in $[pyH]_2[Cu(py)_4(NbOF_5)_2]$ to C_1 by decreasing the predicted ∠O1−Nb−F5 bond angle from 180° to 177.7(1)°, with the apex of the angle directed toward F4. This symmetry-breaking effect is also observed in the helical chain compound $Cu(dpa)_2NbOF_5 \cdot 2H_2O$ (dpa = dipyridylamine).[5] See Supporting Information. In $Cu(dpa)_2NbOF_5 \cdot 2H_2O$, hydrogen bonds are made to both the *trans*-fluoride and one equatorial fluoride, which lengthens the equatorial Nb−F1 bond to 1.953(1) Å (compared to the other equatorial Nb−F bond distances of 1.928(1) Å × 2 and 1.923(1) Å) and lowers the symmetry of the $[NbOF_5]^{2-}$ anion to C_1. As

(38) Desiraju, G. R.; Steiner, T. *The Weak Hydrogen Bond in Structural Chemistry and Biology*; Oxford University Press: New York, 1999; Vol. 9.

in the cluster compounds, the oxide of $[NbOF_5]^{2-}$ in $Cu(dpa)_2NbOF_5 \cdot 2H_2O$ occupies a bridging position between niobium and copper; the Nb═O bond length is 1.760(1) Å with a bond valence of 1.50. The bond angle between the oxide and *trans*-fluoride is ∠O1−Nb−F5 = 178.9(1)° directed toward F1, in contrast to the oxide and *trans*-fluoride bond angles in both $[pyH]_2[Cu(py)_4(NbOF_5)_2]$ and $[4\text{-}apyH]_2[Cu(4\text{-}apy)_4(NbOF_5)_2]$, which are both symmetry fixed at 180°.

Linear Chain Structure of $Cd(3\text{-}apy)_4NbOF_5$. Owing to the *trans*-coordinating nature of the $[NbOF_5]^{2-}$ anion, linear chains that incorporate $[NbOF_5]^{2-}$ can exhibit two different "patterns" of local ordering. In the first pattern, which is optimal for the targeted synthesis of noncentrosymmetric polar materials, the $[NbOF_5]^{2-}$ groups are all aligned in the same manner as shown in Figure 2a for $Cd(3\text{-}apy)_4NbOF_5$. As a result, linear chains with this local ordering possess a net dipole moment since the dipoles from individual $[NbOF_5]^{2-}$ units combine in an additive manner. A second option for local ordering involves chains in which the dipole from one $[NbOF_5]^{2-}$ anion is canceled by the dipole of another anion bonded to the same Cd^{2+}. This configuration would result in two crystallographically distinct Cd^{2+} sites, one that is bonded to the oxides of two $[NbOF_5]^{2-}$ anions (similar to the local bonding environment of the Cu^{2+} ion in the $[pyH]_2[Cu(py)_4(NbOF_5)_2]$ cluster shown in Supporting Information) and one that is bonded to two *trans*-fluorides. Finally, linear chains can also be crystallographically disordered in the oxide/*trans*-fluoride sites. Compounds with this ligand disorder are also nonpolar.

The $Cd(3\text{-}apy)_4NbOF_5$ chain is a rare example of a linear chain compound that is composed of crystallographically ordered $[NbOF_5]^{2-}$ anions. This ordering can be attributed to an extensive bond network that affects five of the six ligands coordinated to Nb^{5+}. The equatorial fluorides of the $[NbOF_5]^{2-}$ anion in $Cd(3\text{-}apy)_4NbOF_5$ participate in more interactions with the hydrogen bond network than in either $[HNC_6H_6OH]_2[Cu(py)_4(NbOF_5)_2]$ or $Cu(dpa)_2NbOF_5 \cdot 2H_2O$. See Figures 4b and Supporting Information. Additionally, each $[NbOF_5]^{2-}$ anion in $Cd(3\text{-}apy)_4NbOF_5$ forms bonds to Cd^{2+} through both the oxide and *trans*-fluoride.

A comparison of the $Cd(3\text{-}apy)_4NbOF_5$ chain structure to the cadmium analogue[3] of the $[pyH]_2[Cu(py)_4(NbOF_5)_2]$ cluster is particularly useful when trying to understand the effects of Cd^{2+} coordination to both the oxide and *trans*-fluoride in $[NbOF_5]^{2-}$. In $[pyH]_2[Cd(py)_4(NbOF_5)_2]$, the Cd−O bond is 2.333(6) Å; this distance is slightly shorter at 2.278(3) Å in $Cd(3\text{-}apy)_4NbOF_5$, indicating a stronger Cd−O bond. At the same time, bond valence calculations shown in Tables 2 and 3 indicate that the Nb═O bond is less covalent in the linear chain compound than that in the $[pyH]_2[Cd(py)_4(NbOF_5)_2]$ cluster. This comparison of the relative bond strength in clusters versus chains will be examined in further detail below. In chains of $Cd(3\text{-}apy)_4NbOF_5$, the *trans*-fluoride appears to compensate for the low bond valence of the Nb═O bond by forming a shorter and stronger bond with the Nb^{5+} than it does in the cluster. Additionally, the equatorial fluorides are not significantly lengthened, but the extensive hydrogen bond network that surrounds the anion reduces the symmetry of $[NbOF_5]^{2-}$ to C_1. Overall, the movement of Nb^{5+} out of the plane defined by the four equatorial fluorides of the $[NbOF_5]^{2-}$ anion (i.e., the primary distortion) is small in the $Cd(3\text{-}apy)_4NbOF_5$ linear chain compound with out-of-plane angles of ∠F2−Nb−F4 = 178.7(1)° and ∠F3−Nb−F5 = 178.1(2)° compared to 169.3(2)° and 166.7(2)° in $[pyH]_2[Cd(py)_4(NbOF_5)_2]$.

Table 4. Average Calculated Mulliken Charges[a] for Uncoordinated $[NbOF_5]^{2-}$ with DFT-Optimized Coordinates, $[pyH]_2[Cd(py)_4(NbOF_5)_2]$, and $Cd(3\text{-}apy)_4NbOF_5$

	$[NbOF_5]^{2-}$	$[pyH]_2[Cd(py)_4(NbOF_5)_2]$	$Cd(3\text{-}apy)_4NbOF_5$
O	−0.842	−0.916	−0.920
F-*trans*	−0.666	−0.637	−0.557
F-*equat*	−0.580	−0.545	−0.537
Nb	+1.826	+1.874	+1.808
Cd		+0.980	+0.883

[a] SCF convergence limit = 0.001.

Electronic Structure of $[NbOF_5]^{2-}$. In an earlier paper,[24] the results of geometry optimizations on an uncoordinated $[NbOF_5]^{2-}$ anion using density functional theory were reported. One of the main advantages of studying uncoordinated $[NbOF_5]^{2-}$ is that it allows for analysis of the primary out-of-center octahedral distortion of the $[NbOF_5]^{2-}$ anion without interference from extended lattice interactions that can induce a secondary distortion. Furthermore, an analysis of the bonding and calculated atomic charges of the idealized $[NbOF_5]^{2-}$ unit is effective for characterizations of the electronic structure and bonding in related compounds. In this section, a brief analysis of the electronic structure of the idealized $[NbOF_5]^{2-}$ anion is presented. This is then used to indicate how the localized Nb═O and Nb−F bonding differs within $[pyH]_2[Cd(py)_4(NbOF_5)_2]$ clusters and $Cd(3\text{-}apy)_4NbOF_5$ chains.

A calculated energy level diagram for an uncoordinated $[NbOF_5]^{2-}$ anion with idealized geometry is shown in the Supporting Information. This diagram indicates that the highest occupied molecular orbitals (i.e., the frontier orbitals) for the idealized $[NbOF_5]^{2-}$ anion are composed primarily of the two O 2p orbitals that are oriented for π bonds with the Nb atom. At the same time, the calculated Mulliken charges listed in Table 4 indicate that the oxide is the most negatively charged ligand, followed by the *trans*-fluoride. Together, these two factors suggest that the $[NbOF_5]^{2-}$ anion is most likely to coordinate through the oxide ligand. The *trans*-fluoride ligand, which contributes strongly to the next highest group of occupied molecular orbitals in $[NbOF_5]^{2-}$, is also a likely site for coordination to a positively charged species. These results are in agreement with previous analyses of $[NbOF_5]^{2-}$ that characterize the anion as *trans*-coordinating through the oxide and *trans*-fluoride ligands on the basis of the overall negative charge distribution.[6,18]

The relative covalent strengths of the Nb−F and Nb═O bonds in $[NbOF_5]^{2-}$ can be quantitatively compared by examining calculated bond overlap populations. Bond overlap populations are a measure of the strength of covalent interactions between two atoms; larger overlap populations correspond to more strongly covalent bonds.[27] The overlap

Table 5. Overlap Populations[a] for Selected Bonds in Uncoordinated $[NbOF_5]^{2-}$ Anions with DFT-Optimized Coordinates, the $[pyH]_2[Cd(py)_4(NbOF_5)_2]$ Cluster Compound, and Linear Chains of $Cd(3\text{-apy})_4NbOF_5$

	$[NbOF_5]^{2-}$	$[pyH]_2[Cd(py)_4(NbOF_5)_2]$	$Cd(3\text{-apy})_4NbOF_5$
Nb−O	0.940	0.863	0.783
Nb−O(σ)	0.420	0.399	0.402
Nb−O(π)	0.520	0.463	0.380
Nb−F *(trans)*	0.317	0.347	0.390
Nb−F(σ)	0.235	0.257	0.273
Nb−F(π)	0.081	0.090	0.117
Nb−F *(equat)*	0.407	0.455	0.463
Cd−O		0.117	0.153
Cd−O(σ)		0.129	0.167
Cd−O(π)		−0.012	−0.014
Cd−F			0.058
Cd−F(σ)			0.066
Cd−F(π)			−0.008

[a] SCF convergence limit = 0.001.

populations for $[NbOF_5]^{2-}$ listed in Table 5 indicate that the Nb═O bond is stronger than the bonds between the Nb^{5+} and the equatorial fluorides, which are, in turn, stronger than the trans Nb−F bond. At first, this observation that the oxide ligand forms the most covalent bond with the central Nb^{5+} ion seems contradictory with the results mentioned earlier that designate the oxide as the most negative ligand in the anion; however, an oxygen atom can accept up to two electrons from a less electronegative species, whereas fluorine can only accept one. Thus, even though oxide carries a greater negative charge than the fluoride ligands in uncoordinated $[NbOF_5]^{2-}$, this charge represents a smaller fraction of the maximum possible charge that can be localized on an oxygen atom.

In addition to comparisons of overall covalent bond strength, overlap populations can provide quantitative information about the σ and π contributions to a particular bond. When the $[NbOF_5]^{2-}$ anion is aligned to a regular Cartesian coordinate system in the same manner as that of our energy level diagram, the O and *trans*-F 2s and $2p_z$ orbitals are oriented for σ-only interactions with Nb orbitals, while the $2p_x$ and $2p_y$ orbitals form π bonds with the niobium. The amount of σ or π character in a metal−ligand bond can be assessed by tabulating the individual valence−orbital overlap populations between the two atoms. The data in Table 5 show, as expected, that π interactions make a significant contribution to the overall strength of the Nb═O bond. In contrast, the more electronegative *trans*-fluoride forms a weaker bond to the Nb^{5+} that is primarily σ bonding in nature.

Lattice Effects on the Electronic Structure of $[NbOF_5]^{2-}$. In this section, the ways in which the electronic structure of the idealized $[NbOF_5]^{2-}$ anion changes as it is incorporated into different crystal structures are analyzed. For example, in the $[pyH]_2[Cd(py)_4(NbOF_5)_2]$ cluster referred to earlier, the $[NbOF_5]^{2-}$ groups are coordinated through the oxide ligands to a late transition metal cation and participate in hydrogen bonding with $[pyH]^+$ units through the fluoride ligands. In linear chain compounds such as $Cd(3\text{-apy})_4NbOF_5$, however, both the oxide and *trans*-fluoride ligands participate

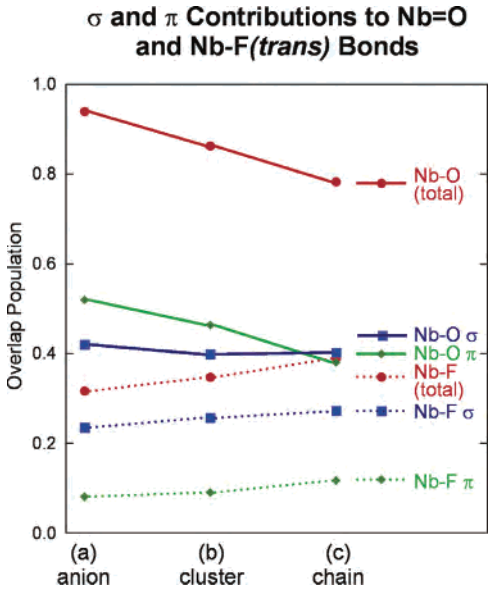

Figure 6. Comparison of the relative Nb═O and trans Nb−F bond strengths (based on calculated bond overlap populations), as well as the σ and π contributions to each, in (a) uncoordinated $[NbOF_5]^{2-}$, (b) the $[pyH]_2[Cd(py)_4(NbOF_5)_2]$ cluster compound, and (c) linear chains of $Cd(3\text{-apy})_4NbOF_5$.

in bridging covalent bonding. The simultaneous increase in Nb═O bond length and decrease in trans Nb−F bond length that is observed experimentally in linear chains relative to cluster compounds indicates that, as the number of covalent bond contacts made by the $[NbOF_5]^{2-}$ group increases, the magnitude of the primary distortion decreases. Results of the calculations presented here support this observation and reveal that different coordination environments have a significant effect on the local bonding within the $[NbOF_5]^{2-}$ anion.

To form the $[pyH]_2[Cd(py)_4(NbOF_5)_2]$ cluster compound, the oxide ligands on two $[NbOF_5]^{2-}$ anions must form bonds with a Cd^{2+} cation. In chains of $Cd(3\text{-apy})_4NbOF_5$, both the oxide and the *trans*-fluoride ligands of a single $[NbOF_5]^{2-}$ unit form bonds to a Cd^{2+} cation. The bond overlap populations given in Table 5 indicate that this Cd−O/Cd−F bond formation occurs directly at the expense of the Nb═O bonding within the compound. Of the four compounds listed in Table 5, the highest Nb═O bond overlap population occurs in the uncoordinated DFT geometry optimized $[NbOF_5]^{2-}$ anion, followed by the $[pyH]_2[Cd(py)_4(NbOF_5)_2]$ cluster. The linear chain compounds, which have higher Cd−O bond overlap populations than the cluster, exhibit the most weakened Nb═O bonding.

A graphical description of the changes in Nb═O and trans Nb−F bond strength within $[NbOF_5]^{2-}$ units is shown in Figure 6. This figure shows that, as the coordination number of the $[NbOF_5]^{2-}$ anion increases (from a to c in Figure 6), the steady weakening of the Nb═O interaction is due almost solely to a loss of π bonding. This finding is particularly significant since, as stated earlier, the primary octahedral distortion of $[NbOF_5]^{2-}$ is typically attributed to $d\pi-p\pi$ bonding interactions between the metal center and the oxide ligand.[2] The loss of Nb═O π bonding is consistent with the decrease in observed primary distortion of the $[NbOF_5]^{2-}$

octahedra when an uncoordinated anion is compared to anions in a cluster and within a linear chain. The Nb═O stretching frequencies in the infrared spectrum show a parallel trend as the double bond character decreases; the short Nb═O bond in $[4\text{-apyH}]_2[Cu(4\text{-apy})_4(NbOF_5)_2]$ shows up at 916 cm^{-1}, while the longer bond in $Cd(3\text{-apy})_4NbOF_5$ appears at 890 cm^{-1}.

The Lewis acid/base adduct $Hg_3(NbF_5)_2SO_4$[39] is an excellent example where the coordination of the niobium atom is completed by one long oxygen bond contact from the sulfate ion. As a result, the Nb−O bond distance is 2.059(13) Å, significantly longer than it is in any of the examples where an out-of-center distortion of a $[NbOF_5]^{2-}$ anion is observed. Correspondingly, the five Nb−F bonds are short, in the range of 1.835−1.899 Å, maintaining an atomic valence of 5 on niobium.

$[NbOF_5]^{2-}$ Order Within $Cd(3\text{-apy})_4NbOF_5$. Unlike $[HNC_6H_6OH]_2[Cu(py)_4(NbOF_5)_2]$ and $Cu(dpa)_2NbOF_5\cdot 2H_2O$, chains of $Cd(3\text{-apy})_4NbOF_5$ are affected by more than one bond network contact that decreases the local symmetry of the $[NbOF_5]^{2-}$ anions. In addition to the asymmetrical hydrogen bond network to the equatorial fluorides, which creates three directional components to the primary distortion, bond overlap populations (Table 5) show that the Cd−O and Cd−F bonds are asymmetric in strength. While this difference in strength is not as extreme as in a cluster, where the difference is between one M−O bond and one hydrogen bond, it still adds two more directional components to the distortion of the anion. Therefore, with a total of five directional components affecting the distortion of the $[NbOF_5]^{2-}$ anion in $Cd(3\text{-apy})_4NbOF_5$, the resultant out-of-center displacement of the Nb^{5+} ion is moderated, but the overall valence on niobium remains well below 5. The presence of five asymmetric bond network contacts ensures that the $[NbOF_5]^{2-}$ anion crystallizes in only one orientation.

It is somewhat surprising that the $[NbOF_5]^{2-}$ ions in $Cd(3\text{-apy})_4NbOF_5$ exhibit a polar crystallographic ordering along the individual chains, particularly when $[NbOF_5]^{2-}$ anions coordinate to the Cd^{2+} cations in a nonpolar manner in $[pyH]_2[Cd(py)_4(NbOF_5)_2]$ clusters. This observation appears to be related to the electron-donating nature of the nitrogen-containing organic ligands around Cd^{2+} and, in turn, to the hard/soft mismatch between Cd^{2+} and O^{2-}/F^- ligands.[40,41] The 3-aminopyridine ligand is more electron donating than unsubstituted pyridine. Correspondingly, the cadmium carries a less positive charge in $Cd(3\text{-apy})_4NbOF_5$ than it does in the $[pyH]_2[Cd(py)_4(NbOF_5)_2]$ cluster, as shown by the calculated Mulliken charges in Table 4. This decrease in charge "softens" the cadmium, making it more prone to participate in covalent bonds than ionic interactions. As a result, the already substantial hard/soft mismatch between the metal and the hard oxide or harder *trans*-fluoride ligands on the $[NbOF_5]^{2-}$ anions is increased. When the $[NbOF_5]^{2-}$ anions order in a polar manner within chains of $Cd(3\text{-apy})_4NbOF_5$, the possibility of an unfavorable F−Cd−F linkage is avoided.

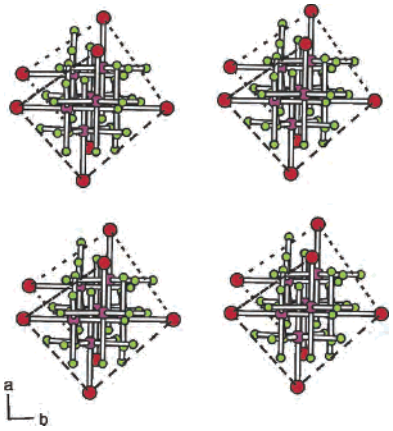

Figure 7. Chirality within the $Cd(3\text{-apy})_4NbOF_5$ structure. The dashed line connects the oxide ligands and is included to illustrate the path of rotation of the $[NbOF_5]^{2-}$ anion as viewed down the *c* axis. The $Cd(3\text{-apy})_4^{2+}$ cations have been removed for clarity.

The chiral component of the $Cd(3\text{-apy})_4NbOF_5$ structure is created by a 4_3-screw axis that is aligned parallel to the *c* axis. The infinite polar sheets of $Cd(3\text{-apy})_4NbOF_5$ chains that are orthogonal to the screw axis rotate in a unidirectional fashion along the screw axis. See Figure 7. The calculated dipole moment[42] of the $[NbOF_5]^{2-}$ anion in $Cd(3\text{-apy})_4NbOF_5$ is 0.56 D. In contrast, the dipole moment of the strongly distorted $[NbOF_5]^{2-}$ anion in $[4\text{-apyH}]_2[Cu(4\text{-apy})_4(NbOF_5)_2]$ is 1.48 D. As the polar sheets of $Cd(3\text{-apy})_4NbOF_5$ rotate along the screw axis, the polar components of the $[NbOF_5]^{2-}$ anions cancel in the *a* and *b* directions, leaving only a small resultant vector in the *c* axis direction. The polar component of the structure is largely due to the Nb−F4 bond that is lengthened by the hydrogen bond network. On the basis of the polar nature of the compound, a small SHG response is expected from $Cd(3\text{-apy})_4NbOF_5$; however, because of the partial radial cancellation of the dipole, the SHG powder efficiency of the sample is below the detection limit of the system, which is about 50% of SiO_2 $\langle d^{2\omega}_{ijk}(SiO_2) = 0.28$ pm/V$\rangle$.[23,43,44]

Crystal Packing in Disordered Linear Chains of $Cu(3\text{-apy})_4NbOF_5$. The linear chain compound $Cu(3\text{-apy})_4NbOF_5$ has a one-dimensional structure similar to that of $Cd(3\text{-apy})_4NbOF_5$, but the oxide and *trans*-fluoride positions of the $[NbOF_5]^{2-}$ anion are crystallographically disordered. Hydrogen bonds are made to each of the four equatorial fluorides from the three-dimensional extended structure, but unlike the hydrogen bonds in $Cd(3\text{-apy})_4NbOF_5$, each hydrogen bond donor is symmetrically arranged around the anion. These contacts symmetrically lengthen the Nb−F bonds, as seen in $[4\text{-apyH}]_2[Cu(4\text{-apy})_4(NbOF_5)_2]$, but are ineffective at ordering the anion. The symmetrical hydrogen

(39) Brown, I. D.; Gillespie, R. J.; Morgan, K. R.; Sawyer, J. F.; Schmitt, K. J.; Tun, Z.; Ummat, P. K.; Vekris, J. E. *Inorg. Chem.* **1987**, *26*, 689−693.
(40) Pearson, R. G. *Chemical Hardness*; John Wiley & Sons: New York, 1997.
(41) Becker, C.; Kieltsch, I.; Broggini, D.; Mezzetti, A. *Inorg. Chem.* **2003**, *42*, 8417−8429.
(42) Maggard, P. A.; Nault, T. S.; Stern, C. L.; Poeppelmeier, K. R. *J. Solid State Chem.* **2003**, *175*, 27−33.
(43) Miller, R. C. *Appl. Phys. Lett.* **1964**, *5*, 17−19.
(44) Jerphagnon, J.; Kurtz, S. K. *Phys. Rev. B: Solid State* **1970**, *3*, 1739−1744.

bond network is unable to reduce the symmetry of the anion, and crystallographic disorder occurs.

The difference between the three-dimensional crystal packing of $Cd(3\text{-apy})_4NbOF_5$ and $Cu(3\text{-apy})_4NbOF_5$ is notable, considering the similarities between their one-dimensional chain structures. Crystal growth occurs in a way that optimizes the intermolecular interactions within a system. Single-crystal X-ray diffraction allows us to study some of the stronger, more easily observed intermolecular interactions such as the electrostatic hydrogen bond. A general rule for hydrogen bonds is that the maximum number of hydrogen bond donor/acceptor pairs will be made.[45] According to Pauling's rules,[46] the most stable coordination sphere is one where the four equatorial fluoride bonds should be approximately equal in length.[47] Both $Cu(3\text{-apy})_4NbOF_5$ and $Cd(3\text{-apy})_4NbOF_5$ have a 2:1 ratio of available amine hydrogens to electronegative acceptors (equatorial fluorides); at a minimum, all four equatorial fluorides should form at least one hydrogen bond. $Cu(3\text{-apy})_4NbOF_5$ does form one hydrogen bond to each available acceptor as predicted. Symmetric lengthening of the equatorial fluorides in $Cu(3\text{-apy})_4NbOF_5$ is observed, and the Nb−F bonds remain isotropic. The equatorial fluorides are also equivalent, but shorter, in structures where no hydrogen bonding occurs.

Unlike $Cu(3\text{-apy})_4NbOF_5$, $Cd(3\text{-apy})_4NbOF_5$ uses three of four available hydrogen bond acceptors. While two fluorides are able to make two hydrogen bond contacts, there is no available hydrogen with which F4 can hydrogen bond. The asymmetrical hydrogen bond environment around the equatorial fluoride positions leads to an anion with reduced symmetry. Bond angles around cadmium in the $Cd(3\text{-apy})_4NbOF_5$ structure deviate from the expected values of 90° with angles between the ring nitrogens at ∠N1−Cd−N3 = 96.4°, ∠N3−Cd−N5 = 83.6°, ∠N5−Cd−N7 = 96.4°, and ∠N1−Cd−N7 = 83.8°. Corresponding angles in $Cu(3\text{-apy})_4NbOF_5$ are ∠N1−Cu−N3 = 89.5° and 90.5°.

In linear chain compounds, disorder between the oxide and *trans*-fluoride elongates the niobium ellipsoid along the Nb−O/F bond axis and is an indication of the anisotropic Nb═O and Nb−F bond lengths. See Figure 1b. The thermal ellipsoid for the $M(L)_4^{2+}$ cation is typically spherical.[4,11] Elongation of the copper thermal ellipsoid in $Cu(3\text{-apy})_4NbOF_5$ along the Cu−O/F bond axis is, therefore, notable and indicates that the copper moves above and below the plane created by the four coordinated 3-aminopyridine rings. A recent review by Murphy and Hathaway[48] lists many examples of common geometries adopted by Cu^{2+} complexes. This flexibility of Cu^{2+} for different coordination geometries may be responsible for the observed elongation of the Cu^{2+} ellipsoid in $Cu(3\text{-apy})_4NbOF_5$. For example, when the axial bonds lengthen around an octahedrally coordinated copper, the coordination approaches square planar as the distortion becomes pronounced to the extent that loss of axial ligands occurs. The two axial Cu−O/F bonds in $Cu(3\text{-apy})_4NbOF_5$ are long at 2.532(1) Å × 2. Previous work has hypothesized that disordered chain structures are actually made up of locally ordered chains where all the dipoles from individual $[NbOF_5]^{2-}$ anions are aligned in an additive manner. Antiparallel packing of such chains would lead to crystallographic disorder.[12,13] If this is the case for $Cu(3\text{-apy})_4NbOF_5$, there should be one oxide and one fluoride coordinated to each $Cu(3\text{-apy})_4^{2+}$ cation, resulting in an anisotropic coordination environment around the Cu^{2+} center. It is reasonable to assume that the resulting Cu−O bond would be stronger than the Cu−F; thus the local bonding around the Cu^{2+} center can be envisioned as a pseudo square pyramid, where Cu^{2+} moves closer to the "apical" O^{2-} ligand and is surrounded by a basal plane of four N atoms from the 3-apy ligands. Interchain disorder would thus account for the elongated Cu^{2+} ellipsoid and the appearance of a distorted octahedral environment around Cu^{2+}.

Conclusions

The observed distortions of d^0 transition metal centered $[MO_nF_{6-n}]^{2-}$ anions are a result of both intraoctahedral interactions and interactions of the anions with their surroundings. The electronic, or primary, distortion is a result of $d\pi-p\pi$ metal−oxide orbital interactions. This distortion is inherent to the oxide fluoride anions and is not a result of contacts with the extended structure (bond network). Secondary distortions, which arise from interactions with the bond network, influence the directionality of the out-of-center distortion and can modify the primary distortion.

When all six ligands on the oxide fluoride anion are crystallographically ordered, the different components that govern the net out-of-center distortion can be identified. Cluster compounds and the linear chain compound $Cd(3\text{-apy})_4NbOF_5$ are comprised of ordered $[NbOF_5]^{2-}$ anions alternating with $M(L)_4^{2+}$ cations ($M = Cd^{2+}, Cu^{2+}$; L = py, 3-apy, 4-apy). The crystal structures reported here illustrate the reduction of the primary distortion when a secondary distortion is detectable. The results of electronic structure calculations support this observation by quantifying the loss of π character in the Nb═O bond as coordination to the anion increases. The observed local coordination environment of the $[NbOF_5]^{2-}$ anions in linear chains of $Cd(3\text{-apy})_4NbOF_5$ differs from those found in discrete cluster compounds, such as $[pyH]_2[Cu(4\text{-apy})_4(NbOF_5)_2]$, and in linear chain compounds with crystallographic disorder in the oxide and *trans*-fluoride bridging positions, as in $Cu(3\text{-apy})_4NbOF_5$. Thus, characterization of $Cd(3\text{-apy})_4NbOF_5$ chains provides an uncommon opportunity to examine the relationship between inherent primary distortions of the $[NbOF_5]^{2-}$ anion and distortions that are induced by the extended hydrogen bonding network.

(45) Etter, M. C. *J. Am. Chem. Soc.* **1982**, *104*, 1095−1096.
(46) Pauling, L. *J. Am. Chem. Soc.* **1929**, *51*, 1010−1026.
(47) Brown, I. D. *Acta Crystallogr. Sect. B* **1992**, *48*, 553−572.
(48) Murphy, B.; Hathaway, B. *Coord. Chem. Rev.* **2003**, *243*, 237−262.

Acknowledgment. We thank Professor P. Shiv Halasyamani at the University of Texas - Houston for the SHG measurement of $Cd(3\text{-apy})_4NbOF_5$ and Drs. Frederick P. Arnold and Margaret E. Welk for valuable insight and discussions. We gratefully acknowledge the support from the National Science Foundation (Solid State Chemistry Award Nos. DMR-9727516 and DMR-0312136) and the use of the Central Facilities supported by the MRSEC program of the National Science Foundation (DMR-0076097) at the Materials Research Center of Northwestern University.

Supporting Information Available: Three X-ray crystallographic files in CIF format including crystallographic details, atomic coordinates, anisotropic thermal parameters, interatomic distances, and angles; a spread sheet with example dipole moment calculations of $[NbOF_5]^{2-}$, infrared spectra, figures of $[pyH]_2[Cu(py)_4(NbOF_5)_2]$, $[HNC_6H_6OH]_2[Cu(py)_4(NbOF_5)_2]$, and $Cu(dpa)_2NbOF_5 \cdot 2H_2O$, and an energy diagram of the $[NbOF_5]^{2-}$ anion, input atomic coordinates in PDF format. This material is available free of charge via the Internet at http://pubs.acs.org.

IC048766D